ACS SyntheticBiology

Letter

pubs.acs.org/synthbio

Programming Membrane Fusion and Subsequent Apoptosis into Mammalian Cells

Seema Nagaraj,[†] Evan Mills,[†] Stanley S. C. Wong,[†] and Kevin Truong*[,†,‡]

[†]Institute of Biomaterials and Biomedical Engineering, University of Toronto, 164 College Street, Toronto, Ontario, M5S 3G9, Canada

[‡]Edward S. Rogers, Sr. Department of Electrical and Computer Engineering, University of Toronto, 10 King's College Circle, Toronto, Ontario, M5S 3G4, Canada

Supporting Information

ABSTRACT: By the delivery of specific natural or engineered proteins, mammalian cells can be programmed to perform increasingly sophisticated and useful functions. Here, we introduce a set of proteins that has potential value in cell-based therapies by programming a cell to target tumor cells. First, the delivery of VSV-G (vesicular stomatitis virus glycoprotein) allowed the cell to undergo membrane fusion with adjacent cells to form syncytia (i.e., a multinucleated cell) in conditions of low pH typically occurring at a tumor site. The formation of syncytia caused the clustering of nuclei along with an integration of the microtubule network and ER. Interestingly, the formation of syncytia between cells that are dynamically blebbing, a mode of migration preferred during tumor metastasis, resulted in the loss of these morphology changes. Lastly, the codelivery of VSV-G with L57R (an engineered photoactivated caspase-7) allowed cells to undergo low pH-dependent membrane fusion followed by blue light-dependent apoptosis. In cell-based therapies, the clearance of syncytia between tumor cells might further trigger an immune response against the tumor.

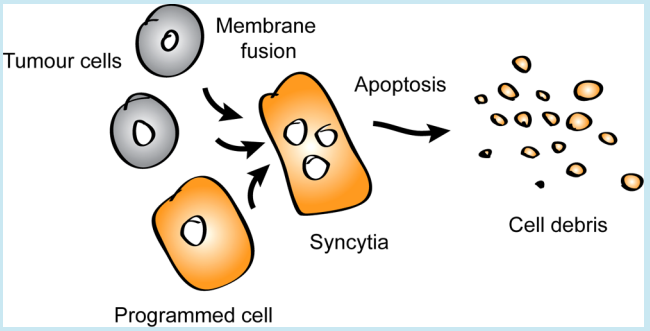

KEYWORDS: *synthetic biology, cellular programming, membrane fusion, apoptosis*

Cells can be programmed to perform a diverse set of functions through the delivery of natural or engineered proteins. This concept has been applied notably to the reprogramming of stem cell fate by delivering a set of transcription factors for converting mouse fibroblasts to pluripotent stem cells, neurons[1] or cardiomyocytes.[2] Cellular programming can be applied more broadly to control not just stem cell fate but cell behavior. While most applications to date have used naturally occurring proteins, the efforts to engineer proteins expand the possibilities of rewiring biological functions. For instance, through protein engineering with the LOV2 domain, engineered proteins have brought cell migration,[3] gene transcription,[4] Ca^{2+} entry[5] and apoptosis[6] under the direct control of blue light. Further, the engineering of Ca^{2+} sensitive proteins allows rewiring of many stimuli through the natural modularity of Ca^{2+} signaling.[7] Specifically, through the coexpression of an engineered Ca^{2+} sensitive RhoA with the acetylcholine receptor or channelrhodopsin-2, cell migration could be controlled by acetylcholine and blue light, respectively.[7,8]

Through a network of the natural and engineered genes, programmed cells can begin to perform increasingly sophisticated and useful functions such as the identification of a tumor site, inhibition of metastasis and initiation of tumor cell death. When a solid tumor reaches beyond the size of 1−2 mm^3, the cells in the center of the tumor experience a microenvironment with low oxygen and nutrients.[9,10] Low oxygen, in particular, causes the cell to switch from respiration to glycosis for ATP production that in turn lowers pH around the tumor site.[11,12] To continue its expansion, the tumor grows blood vessels that restore oxygen and nutrient supply (i.e., angiogenesis) and at a later stage, these vessels serve as conduits for tumor cells to migrate to other sites (i.e., metastasis). Thus, new anticancer drugs[13−15] have been developed to target pathways regulating angiogenesis and metastasis, but they too have significant side-effects as these pathways likewise function in normal physiology. An ideal therapeutic could recognize a disease condition and then act locally to minimize systemic side-effects (i.e., similar to the immune system at its best). For instance, a programmed cell could recognize the tumor microenvironment via low pH, inhibit metastasis and then initiate cell death of both the tumor and programmed cell.

Here, we introduce a set of proteins that has potential value in programming a cell for therapeutic intervention against tumor cells. To recognize the low pH environment at the tumor site, vesicular stomatitis virus glycoprotein (VSV-G) was

Received: May 16, 2012
Published: September 18, 2012

   dx.doi.org/10.1021/sb3000468 | *ACS Synth. Biol.* 2013, 2, 173−179

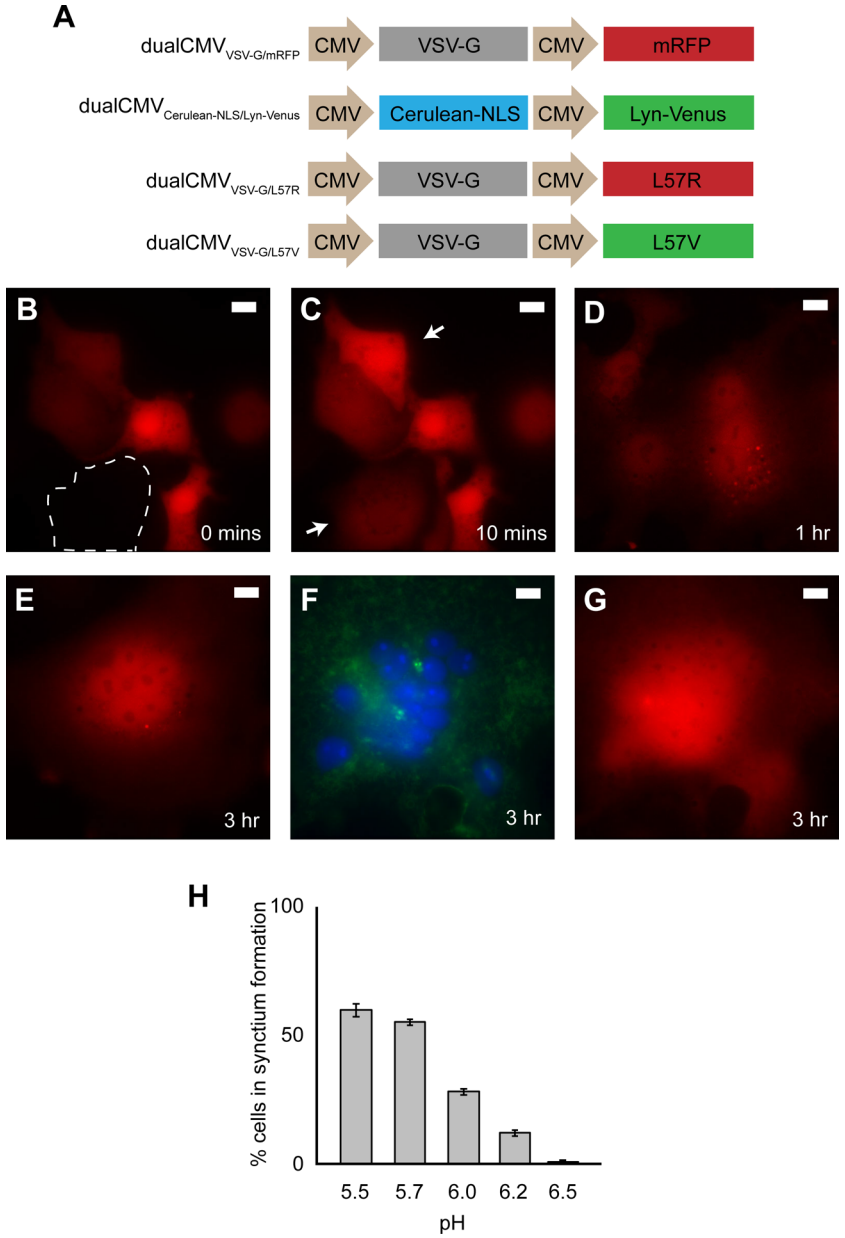

Figure 1. VSV-G facilitates membrane fusion at low pH. (A) Schematic layout of vectors created in the study. (B, C) The fluorescence image of COS-7 cells transfected with dualCMV$_{VSV\text{-}G/mRFP}$ after replacement with PBS (pH 6, 25 °C) at 0 and 10 min. The dotted line indicates the location of an untransfected cell, while the arrows indicate cells that have gained fluorescence or become brighter. (D, E) The fluorescence image of cells incubated in DMEM (pH 7.4, 37 °C, 5% CO_2) after 1 and 3 h. COS-7 cells were cotransfected with dualCMV$_{VSV\text{-}G/mRFP}$ and dualCMV$_{Cerulean\text{-}NLS/Lyn\text{-}Venus}$ and similarly treated for 10 min in PBS (pH 6, 25 °C). (F, G) The fluorescence image of cells after a 3 h incubation in DMEM (pH 7.4, 37 °C, 5% CO_2). Red fluorescence was shown separately so that the nucleus is more visible. (H) Percentage of cells in syncytium formation with different pH buffers. The percentage was calculated as the total number of cells involved in syncytium formation divided by the total number of cells observed (n = 3 experiments). Images are in false color (i.e., blue for Cerulean, green for Venus, red for mRFP). The scale bar is 10 μm. See also Figure S1 (Supporting Information).

used, a common envelope protein employed in lentivirus generation that allows transfection of a wide variety of cell types.[16] When VSV-G was expressed in mammalian cells, we observed membrane fusion between cells when the pH was lowered to ~6 (e.g., a level of acidity found within the tumor site), a finding consistent with the literature.[17,18] The formation of syncytia (i.e., fused cells with 3 or more nuclei) resulted in the gradual clustering of the nuclei and rearrangement of the microtubule network and endoplasmic reticulum (ER). Furthermore, syncytia formation between dynamically blebbing cells resulted in the cessation of blebbing or amoeboid-like cell morphologies, a mode of cell migration preferred during metastatic migration of certain cell types.[19] To initiate death of the syncytia, we used L57R, a previously engineered caspase-7 protein and induced apoptosis by blue light excitation.[6] Apoptosis is a particularly desirable form of cell death because the cells die in an orderly way and then are silently cleared by the immune system in a process that causes no inflammation. During cell clearance, dendritic cells can uptake antigens from the fused cell to initiate a specific immune response against both the tumor and programmed cell.[20]

dx.doi.org/10.1021/sb3000468 | ACS Synth. Biol. 2013, 2, 173−179

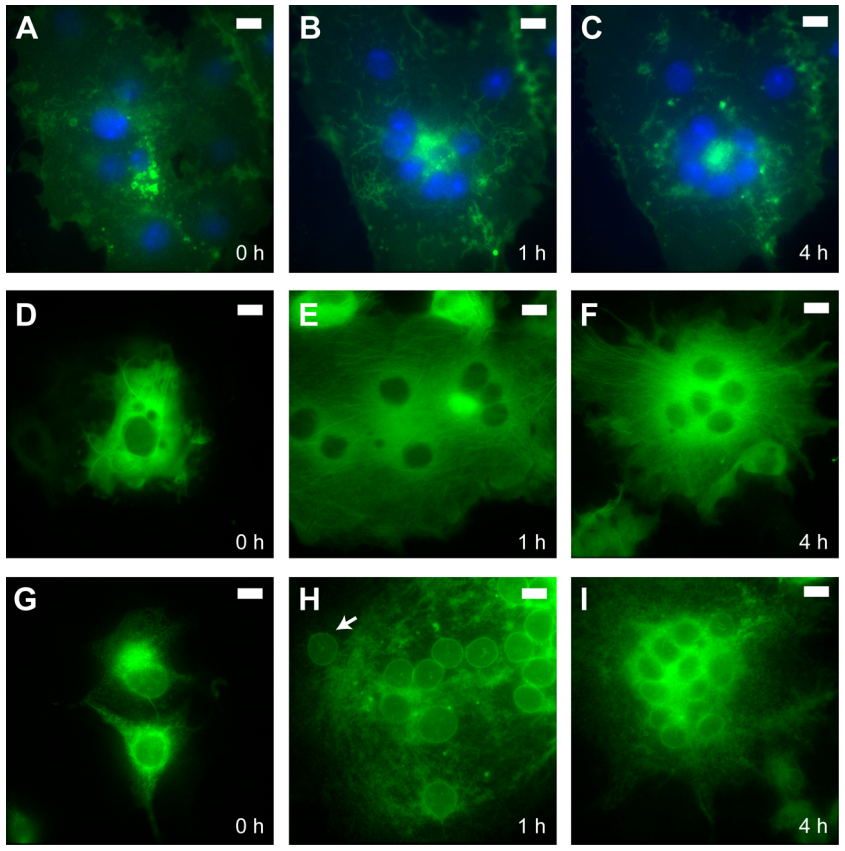

Figure 2. The rearrangement of the nuclei, the microtubule network and ER from syncytia formation. Membrane fusion was induced by treating COS-7 cells for 10 min in PBS (pH 6, 25 °C) and then incubated in DMEM (pH 7.4, 37 °C, 5% CO_2) for 1 h. To observe nuclei changes, COS-7 cells cotransfected with dualCMV$_{VSV\text{-}G/mRFP}$ and dualCMV$_{Cerulean\text{-}NLS/Lyn\text{-}Venus}$ were imaged after (A) 0 h, (B) 1 h and (C) 4 h. To observe microtubule network changes, COS-7 cells cotransfected with dualCMV$_{VSV\text{-}G/mRFP}$ and EB1-GFP were imaged after (D) 0 h, (E) 1 h and (F) 4 h. To observe ER changes, COS-7 cells cotransfected with dualCMV$_{VSV\text{-}G/mRFP}$ and FKBP12-TM$_{TLR4}$-Venus-KDEL were imaged after (G) 0 h, (H) 1 h and (I) 4 h. The arrow in H indicates a nucleus without a surrounding Golgi apparatus. Images are in false color (i.e., blue for Cerulean, green for Venus, red for mRFP). The scale bar is 10 μm. See also Movies S1 and S2 (Supporting Information).

Mammalian cells transfected with VSV-G underwent cell−cell membrane fusion at low pH[17] (n = 30/30 experiments) (Figure 1). To allow expression of two proteins in transfected cells, a dualCMV vector was assembled to contain two CMV promoters with multiple cloning sites. In the dualCMV$_{VSV\text{-}G/mRFP}$ vector, VSV-G expression was controlled by one CMV promoter, while monomeric red fluorescent protein[21] (mRFP) expression was controlled by the other (Figure 1A). COS-7 cells transfected with dualCMV$_{VSV\text{-}G/mRFP}$ had red fluorescence localized to the nucleus and cytoplasm, where the nucleus had a slightly higher fluorescence that excluded the nucleolus (Figure 1B). After 10 min in PBS (pH 6), we noticed a fluorescence redistribution: one cell became brighter and nonfluorescent cells became fluorescent (Figure 1C). This indicated that early membrane fusion occurred in some cells because mRFP could freely diffuse between cells. Next, the media was replaced with DMEM (pH 7.4) and incubated at 37 °C and 5% CO_2. After 1 h, most cells in the culture dish appeared to be fused with 2−3 nuclei (Figure 1D). After 3 h, most cells were giant cells (called syncytia) with greater than 4 nuclei that clustered together (Figure 1E), indicating that membrane fusion can fuse more than 2 cells together.

To more clearly observe the nucleus and plasma membrane, the dualCMV$_{Cerulean\text{-}NLS/Lyn\text{-}Venus}$ vector was created, where Cerulean-NLS is Cerulean[22] (i.e., mutant cyan fluorescent protein) fused with a nuclear localization signal (RIRKKLR) and Lyn-Venus is Venus[23] (i.e., mutant yellow fluorescent protein) fused with the plasma membrane localization signal from Lyn kinase (GCIKSKGKDSA) (Figure 1A). Next, COS-7 cells cotransfected with dualCMV$_{VSV\text{-}G/mRFP}$ and dualCMV$_{Cerulean\text{-}NLS/Lyn\text{-}Venus}$ were similarly induced to fuse membranes by PBS (pH 6). With the nuclear marker, we could clearly observe some cells had greater than 10 nuclei after 3 h (Figure 1F,G). To establish the range of pH required to induce membrane fusion, we determined the percentage of cells involved in syncytia formation in pH buffers varying from 5.5, 5.7, 6.0, 6.2, and 6.5 (Figure 1H). Consistent with previous studies,[17] the membrane fusion occurred negligibly at pH 6.5, moderately at pH 6.2 and readily at 5.5, 5.7, or 6.0. Lastly, low pH-dependent membrane fusion was apparent in all tested mammalian cell lines (i.e., HeLa and HEK293 cells) (Figure S1, Supporting Information).

After cell−cell membrane fusion, the nuclei of the syncytia clustered, along with an integration of the microtubule network and ER. COS-7 cells cotransfected with dualCMV$_{VSV\text{-}G/mRFP}$ and dualCMV$_{Cerulean\text{-}NLS/Lyn\text{-}Venus}$ were fused together in the previous low pH conditions. Initially, the nuclei were separated, and gradually over 3 h, the nuclei began to cluster together, suggesting a dynamic rearrangement of cell structure (Figure 2A−C, Movies S1 and S2, Supporting Information) (n = 10 experiments). To track changes in the microtubule network,

dx.doi.org/10.1021/sb3000468 | ACS Synth. Biol. 2013, 2, 173−179

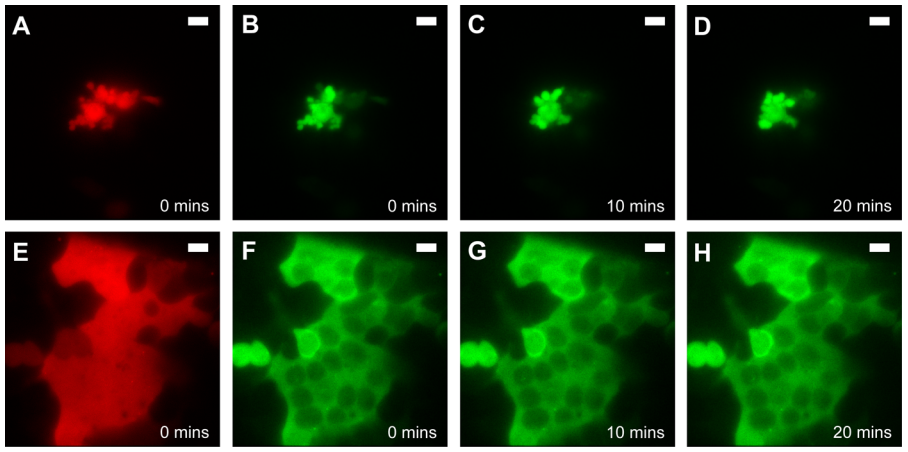

Figure 3. Dynamic blebbing is stopped by syncytia formation. The fluorescence images of HEK293 cells cotransfected with dualCMV$_{VSV\text{-}G/mRFP}$ and RhoA(Q63L)-Venus at (A,B) 0 min, (C) 10 min and (D) 20 min. After membrane fusion, the fluorescence images of HEK293 cells transfected with dualCMV$_{VSV\text{-}G/mRFP}$ and RhoA(Q63L)-Venus at (E,F) 0 min, (G) 10 min and (H) 20 min. Images are in false color (i.e., green for Venus, red for mRFP). The scale bar is 10 μm. See also Movies S3 and S4 (Supporting Information).

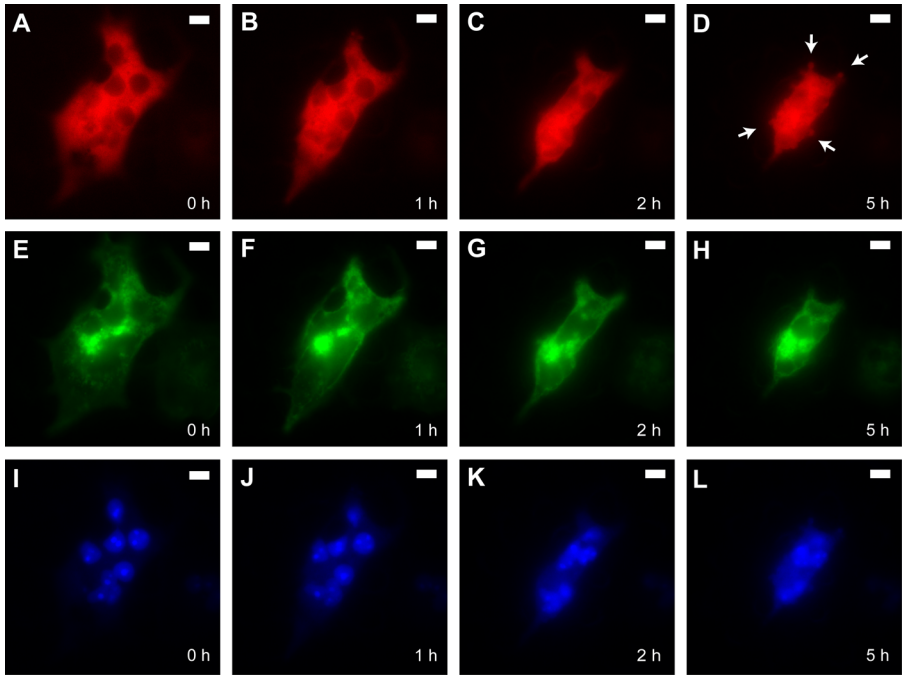

Figure 4. Programming membrane fusion and subsequent apoptosis. Again, membrane fusion was induced by treating COS-7 cells for 10 min in PBS (pH 6, 25 °C) and then incubated in DMEM (pH 7.4, 37 °C, 5% CO_2) for 1 h. The fluorescence images of COS-7 syncytia cotransfected with dualCMV$_{VSV\text{-}G/L57R}$ and dualCMV$_{Cerulean\text{-}NLS/Lyn\text{-}Venus}$ at (A, E, I) 0 h, (B, F, J) 1 h, (C, G, K) 2 h and (D, H, L) 5 h. Images are in false color (i.e., blue for Cerulean, green for Venus, red for mRFP). The scale bar is 10 μm. See also Movies S7–S9 (Supporting Information).

COS-7 cells were cotransfected with dualCMV$_{VSV\text{-}G/mRFP}$ and EB1-GFP[24] (Figure 2D–F) (n = 3 experiments). Ending Binding 1 (EB1) is a highly conserved protein that regulates the growth of microtubules, and when fused with green fluorescent protein (EB1-GFP), it labels growing microtubules during mitosis.[24] Prior to cell–cell membrane fusion, some contorted strands of microtubule fibers were observed in random orientations inside the cell (Figure 2D). The large background fluorescence was from excess EB1-GFP that did not associate with polymerizing microtubules. After cell–cell membrane fusion, many long straight strands of microtubule fibers were observed inside the syncytia (Figure 2E,F). To track changes in the ER, COS-7 cells were cotransfected with dualCMV$_{VSV\text{-}G/mRFP}$ and FKBP12-TM$_{TLR4}$-Venus-KDEL[25] (Figure 2G–I) (n = 3 experiments). FKBP12-TM$_{TLR4}$-Venus-KDEL is a synthetic transmembrane protein designed by our group that labels the ER with Venus, which appears as a web-like fluorescence distribution.[25] There was also a fluorescent outline that defined the nuclear envelope surrounded by a cluster of fluorescence that defined the Golgi apparatus (Figure 2G). After cell–cell membrane fusion, nuclei away from the main cluster of nuclei appear to lose their Golgi apparatus, suggesting that only one area of the syncytia can function as the Golgi apparatus (Figure 2H,I).

The membrane fusion between cells undergoing dynamic blebbing or amoeboid-like morphology changes resulted in the loss of these morphology changes. Blebbing and amoeboid-like migration by RhoA is thought to be the mode of cell motility

dx.doi.org/10.1021/sb3000468 | *ACS Synth. Biol.* 2013, 2, 173–179

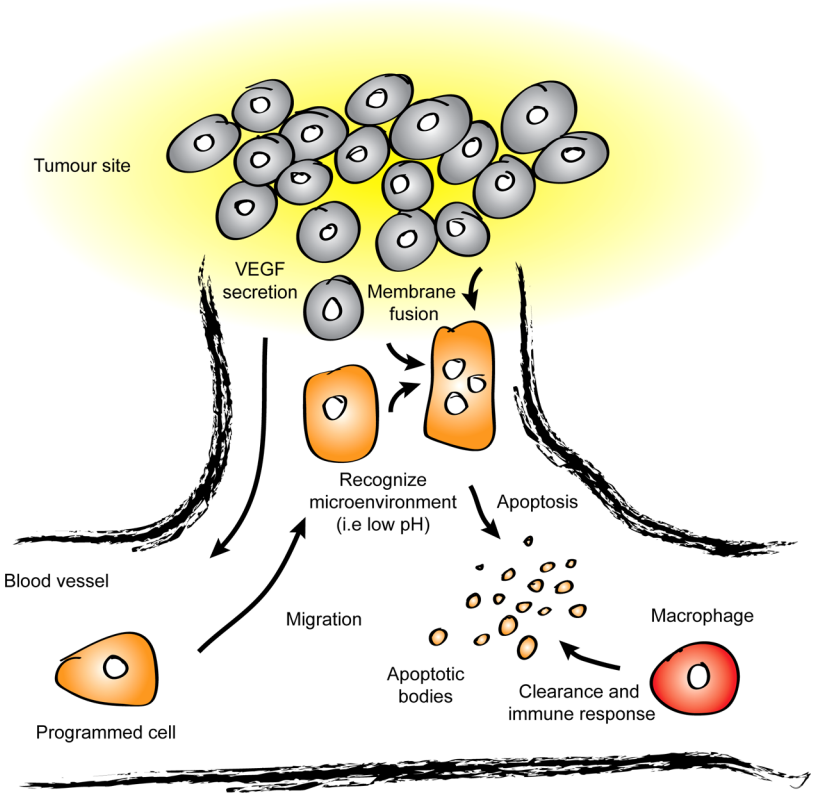

Figure 5. Programming a cell to target and eliminate tumor cells. First, the engineered cell migrates to the tumor site by the signals released by the tumor site (e.g., VEGF). Second, it recognizes the specific microenvironment of the tumor site (e.g., low pH). Third, it initiates membrane fusion with tumor cells to create syncytia. Lastly, it dies by apoptosis and is cleared by the immune system in a process that may trigger a further adaptive immune response against the tumor.

preferred in cancer metastasis of certain cell types, which appear as spherical extensions from cell.[26,27] In weakly adherent cell lines like HEK293, the overexpression of the dominant positive mutant of RhoA (Q63L) induces dynamic cell blebbing that could guide cell migration to close a wound in *in vitro* assays.[7] Thus, HEK293 cells were cotransfected with dualCMV$_{\text{VSV-G/mRFP}}$ and dominant positive RhoA (Q63L) to first induce dynamically blebbing as observed by forming and retracting spherical extensions from the cell (Figure 3A−D, Movie S3, Supporting Information) (n = 3 experiments). After cell−cell membrane fusion induced by low pH, the syncytia no longer displayed any dynamic blebbing (Figure 3E−H, Movie S4, Supporting Information) (n = 3 experiments). Cell−cell membrane fusion was evident as there was relatively uniform fluorescence intensity within the syncytia and a lack of cell boundaries. Lastly, a similar lost of dynamic blebbing was observed in fused HeLa cells overexpressing dominant positive RhoA (Q63L) (Figure S2, Movies S5 and S6, Supporting Information) (n = 3 experiments). The cessation of dynamic blebbing in syncytia should reduce their motility, which is intuitive as increasing size is commonly correlated with decreasing motility.

By coexpressing VSV-G and the engineered protein L57R, mammalian cells were programmed for low pH-dependent membrane fusion and light-dependent apoptosis (Figure 4; Movies S7−S9, Supporting Information) (n = 3 experiments). L57R is a photoactivable caspase-7 engineered by our group through the tandem fusion of the LOV2 domain, the catalytic domain of caspase-7 and mRFP.[6] When stimulated by blue light, the LOV2 releases inhibition of the catalytic domain of caspase-7, allowing it to cleave substrates that execute the apoptosis pathway. The dualCMV$_{\text{VSV-G/L57R}}$ vector was constructed to allow expression of both VSV-G and L57R (Figure 1A). When COS-7 cells were transfected with dualCMV$_{\text{VSV-G/L57R}}$ and induced with low pH conditions, they could efficiently fuse with untransfected cells (Figure S4, Supporting Information). Next, COS-7 cells cotransfected with dualCMV$_{\text{VSV-G/L57R}}$ and dualCMV$_{\text{Cerulean-NLS/Lyn-Venus}}$ were induced to fuse membranes by the previous low pH conditions. Again, the lack of cell boundaries and the relative uniformity of fluorescence within syncytia confirmed that the cell−cell membrane fusion occurred. The nuclei were also detected under red fluorescence since L57R is large enough to be excluded from the nucleus. Since only minimal light stimulation was needed to activate L57R, syncytia were stimulated using a pulsed blue light with a long period and short exposure (i.e., 300 ms exposure every minute) to minimize phototoxicity. After 1 h, there was dramatic shrinkage in syncytia, but nuclei remained distinct. After 2 h, the syncytia began to round and there was nuclear instability as some nuclei disappeared or merged. After 4 h, there was dynamic blebbing in the syncytia. All these changes are consistent with apoptotic cell death mediated by L57R.[6] Using the same blue light excitation in syncytia transfected with dualCMV$_{\text{VSV-G/mRFP}}$ and dualCMV$_{\text{Cerulean-NLS/Lyn-Venus}}$, syncytia had minimal cell morphology changes and no nuclear instability or dynamic blebbing (Figure 2A−C). As expected, blue light excitation of syncytia transfected with dualCMV$_{\text{VSV-G/L57 V}}$ also stained positive for propidium iodide, which labels DNA in dead cells (Figure S3, Supporting Information) (n = 3 experiments).

dx.doi.org/10.1021/sb3000468 | *ACS Synth. Biol.* 2013, 2, 173−179

We have demonstrated a potentially useful set of proteins to program cells to target and eliminate tumor cells (Figure 5). The expression of VSV-G allows a cell to recognize the low-pH environment around a tumor site and then subsequently start membrane fusion to form syncytia with tumor cells. Next, the expression of L57R allows the syncytia between the programmed and tumor cells to undergo photoactivated apoptosis. The subsequent clearance of the syncytia by the immune system can potentially initiate a specific immune response against both the tumor and programmed cell.[20] It is possible that more genes are still necessary to enable the programmed cell to migrate to the tumor site. Since tumor sites secrete growth factors such as vascular endothelial growth factor (VEGF) for angiogenesis,[28] cell migration toward tumor sites can potentially be programmed using a protein network of the VEGF receptor and engineered Ca^{2+} sensitive RhoA proteins.[7,8] For ultimate applications in cell-based therapies, it will be important to study the consequences of creating syncytium with tumor cells as it may result in nuclear fusion, genomic instability and an overall more aggressive tumor. Furthermore, VSV-G dependent membrane fusion may activate prematurely and induce fusion with normal cells to cause off target toxicity. Other issues include determining the best cell type to program along with whether to genetically modify the patient's own cells or a universal cell with immunosuppressants.[29] Nevertheless, membrane fusion combined with apoptosis might be a useful general strategy to clear unwanted cells in cell-based therapies.

MATERIALS AND METHODS

Plasmids. To express two proteins from a single vector, the dualCMV vector was assembled with two CMV promoters and multiple cloning sites using a cassette-based methodology described previously.[30−32] EB1-GFP and VSV-G were from Addgene (Cambridge, MA) plasmids 17234 and 11914, respectively. VSV-G was amplified by PCR and inserted into the pCfvtx vector.[31] All subsequent fusion proteins were subcloned as previously described[30−32] and then inserted into dualCMV vector via compatible restriction endonuclease sites.

Cell Culture and Transfection. COS7, HeLa and HEK293 cells were maintained in Dulbecco's Modified Eagle's Medium (DMEM) containing 25 mM D-glucose, 1 mM sodium pyruvate and 4 mM L-glutamine (Invitrogen, Carlsbad, CA) with 10% supplemented Fetal Bovine Serum (FBS) (Sigma Aldrich, St. Lois, MO) in T5 flasks (37 °C and 5% CO_2). Cells were passaged at 95% confluency using 0.05% Trypsin with EDTA (Sigma) and seeded onto 35 mm glass-bottom dishes (MatTek, Ashland, MA) at 1:15 dilution. Cells were transiently transfected using Lipofectamine 2000 according to manufacturer's protocols (Invitrogen).

Induction of Membrane Fusion. The cell media was replaced with a phosphate buffered saline (PBS) buffer adjusted to pH 6 by addition of hydrochloric acid. After 10 min of incubation at room temperature, the cell media was replaced with DMEM + 10% FBS and incubated 37 °C and 5% CO_2 for 3 h.

Illumination and Imaging. Imaging was performed using an inverted IX81 microscope with Lambda DG4 xenon lamp source and QuantEM 512SC CCD camera with a 60× oil immersion objective (Olympus). Filter excitation (EX) and emission (EM) bandpass specifications were as follows (in nm): CFP (EX: 438/24, EM: 482/32), YFP (EX: 500/24, EM: 542/27), RFP (EX: 580/20, EM: 630/60) (Semrock). Image acquisition was done with MetaMorph Advanced (Olympus).

Quantification of Membrane Fusion in Varying pH Conditions. For each pH condition, three independent experiments were performed. For each experiment, 30 random frames containing transfected cells were collected from the microscope described above. Nonsyncytia were cells that contained 1 or 2 nuclei, whereas syncytia were cells with 3 or more nuclei. Percentage of syncytium formation was calculated by dividing the number of syncytia with the number of cells.

Induction of Photoactivated Apoptosis. Cells transfected with L57R were illuminated for 300 ms every minute using the CFP excitation filter. The light intensity was measured at 25 mW/cm^2.

Propidium Iodide Staining and Imaging. The cell media was replaced with a PBS buffer containing 2 μM of propidium iodide (Sigma). After 5 min, the cell media was replaced with PBS buffer. Fluorescence from propidium iodide was measured using optical filters for RFP described above.

ASSOCIATED CONTENT

Supporting Information

Supporting figures and movies. This material is available free of charge via the Internet at http://pubs.acs.org

AUTHOR INFORMATION

Corresponding Author

*Tel: 416-978-7772. Fax: 416-978-4317 164. E-mail: kevin.truong@utoronto.ca.

Author Contributions

S.N. designed and carried out the experiments, created plasmids used, analyzed the data and helped write the manuscript. E.M. and S.W. produced plasmids used in the work. K.T. conceived the initial idea, analyzed the data and wrote the manuscript.

Notes

The authors declare no competing financial interest.

ACKNOWLEDGMENTS

This work was supported by a grant to K.T. from the Canadian Institutes of Health Research (#81262). Zahra Mirzaei produced the pH buffers.

REFERENCES

(1) Vierbuchen, T., Ostermeier, A., Pang, Z. P., Kokubu, Y., Sudhof, T. C., and Wernig, M. (2010) Direct conversion of fibroblasts to functional neurons by defined factors. *Nature 463*, 1035−1041.

(2) Ieda, M., Fu, J. D., Delgado-Olguin, P., Vedantham, V., Hayashi, Y., Bruneau, B. G., and Srivastava, D. (2010) Direct reprogramming of fibroblasts into functional cardiomyocytes by defined factors. *Cell 142*, 375−386.

(3) Wu, Y. I., Frey, D., Lungu, O. I., Jaehrig, A., Schlichting, I., Kuhlman, B., and Hahn, K. M. (2009) A genetically encoded photoactivatable Rac controls the motility of living cells. *Nature 461*, 104−108.

(4) Strickland, D., Yao, X., Gawlak, G., Rosen, M. K., Gardner, K. H., and Sosnick, T. R. (2010) Rationally improving LOV domain-based photoswitches. *Nat. Methods 7*, 623−626.

(5) Pham, E., Mills, E., and Truong, K. (2011) A synthetic photoactivated protein to generate local or global Ca(2+) signals. *Chem. Biol. 18*, 880−890.

(6) Mills, E., Chen, X., Pham, E., Wong, S. S., and Truong, K. (2012) Engineering a photo-activated caspase-7 for rapid induction of apoptosis. *ACS Synth. Biol. 1*, 75−82.

(7) Mills, E., and Truong, K. (2011) Ca(2+)-mediated synthetic biosystems offer protein design versatility, signal specificity, and pathway rewiring. *Chem. Biol. 18*, 1611−1619.
(8) Mills, E., Pham, E., and Truong, K. (2010) Structure based design of a Ca2+-sensitive RhoA protein that controls cell morphology. *Cell Calcium 48*, 195−201.
(9) Hanahan, D., and Folkman, J. (1996) Patterns and emerging mechanisms of the angiogenic switch during tumorigenesis. *Cell 86*, 353−364.
(10) Kerbel, R. S. (2008) Tumor angiogenesis. *N. Engl. J. Med. 358*, 2039−2049.
(11) Janelle, V., Brassard, F., Lapierre, P., Lamarre, A., and Poliquin, L. (2011) Mutations in the glycoprotein of vesicular stomatitis virus affect cytopathogenicity: potential for oncolytic virotherapy. *J. Virol. 85*, 6513−6520.
(12) Barber, G. N. (2004) Vesicular stomatitis virus as an oncolytic vector. *Viral Immunol. 17*, 516−527.
(13) Wilson, W. R., and Hay, M. P. (2011) Targeting hypoxia in cancer therapy. *Nat. Rev. Cancer 11*, 393−410.
(14) Moschetta, M., Cesca, M., Pretto, F., and Giavazzi, R. (2010) Angiogenesis inhibitors: implications for combination with conventional therapies. *Curr. Pharm. Des. 16*, 3921−3931.
(15) Argiris, K., Panethymitaki, C., and Tavassoli, M. (2011) Naturally occurring, tumor-specific, therapeutic proteins. *Exp. Biol. Med. 236*, 524−536.
(16) Kafri, T. (2004) Gene delivery by lentivirus vectors an overview. *Methods Mol. Biol. 246*, 367−390.
(17) Sun, X., Belouzard, S., and Whittaker, G. R. (2008) Molecular architecture of the bipartite fusion loops of vesicular stomatitis virus glycoprotein G, a class III viral fusion protein. *J. Biol. Chem. 283*, 6418−6427.
(18) Gottesman, A., Milazzo, J., and Lazebnik, Y. (2010) V-fusion: a convenient, nontoxic method for cell fusion. *Biotechniques 49*, 747−750.
(19) Sahai, E., and Marshall, C. J. (2003) Differing modes of tumour cell invasion have distinct requirements for Rho/ROCK signalling and extracellular proteolysis. *Nat. Cell Biol. 5*, 711−719.
(20) Savill, J., Dransfield, I., Gregory, C., and Haslett, C. (2002) A blast from the past: clearance of apoptotic cells regulates immune responses. *Nat. Rev. Immunol. 2*, 965−975.
(21) Campbell, R. E., Tour, O., Palmer, A. E., Steinbach, P. A., Baird, G. S., Zacharias, D. A., and Tsien, R. Y. (2002) A monomeric red fluorescent protein. *Proc. Natl. Acad. Sci. U. S. A. 99*, 7877−7882.
(22) Rizzo, M. A., Springer, G. H., Granada, B., and Piston, D. W. (2004) An improved cyan fluorescent protein variant useful for FRE. *Nat. Biotechnol. 22*, 445−449.
(23) Nagai, T., Ibata, K., Park, E. S., Kubota, M., Mikoshiba, K., and Miyawaki, A. (2002) A variant of yellow fluorescent protein with fast and efficient maturation for cell-biological applications. *Nat. Biotechnol. 20*, 87−90.
(24) Piehl, M., and Cassimeris, L. (2003) Organization and dynamics of growing microtubule plus ends during early mitosis. *Mol. Biol. Cell 14*, 916−925.
(25) Nagaraj, S., Wong, S. S., and Truong, K. (2012) Parts-based assembly of synthetic transmembrane proteins in mammalian cells. *ACS Synth. Biol. 1*, 111−117.
(26) Blaser, H., Reichman-Fried, M., Castanon, I., Dumstrei, K., Marlow, F. L., Kawakami, K., Solnica-Krezel, L., Heisenberg, C. P., and Raz, E. (2006) Migration of zebrafish primordial germ cells: a role for myosin contraction and cytoplasmic flow. *Dev. Cell 11*, 613−627.
(27) Fackler, O. T., and Grosse, R. (2008) Cell motility through plasma membrane blebbing. *J. Cell Biol. 181*, 879−884.
(28) Kerbel, R., and Folkman, J. (2002) Clinical translation of angiogenesis inhibitors. *Nat. Rev. Cancer 2*, 727−739.
(29) Dove, A. (2002) Cell-based therapies go live. *Nat. Biotechnol. 20*, 339−343.
(30) Pham, E., and Truong, K. (2010) Design of fluorescent fusion protein probes. *Methods Mol. Biol. 591*, 69−91.
(31) Truong, K., Khorchid, A., and Ikura, M. (2003) A fluorescent cassette-based strategy for engineering multiple domain fusion proteins. *BMC Biotechnol. 3*, 1−8.
(32) Wong, S. S., and Truong, K. (2010) Fluorescent protein-based methods for on-plate screening of gene insertion. *PLoS One 5*, e14274.